TABLE I. Experimental parameters used in calculations for KI.

E_G	6.34 eV[a]
E_B	0.35[a]
E_{x1}	5.99[a] (true = 5.87)[b]
$\hbar\omega_l$	0.018 (Ref. 6)
Γ_{1s}	0.1[a]
Γ_{2s}	0.087[a]
ϵ_∞	2.82 (b and Ref. 9)
ϵ_s	4.66[c]
M_e	0.398[c]
M_h	0.421
$\alpha'^{(1s)}$ (max)	8×10^5 cm^{-1} [d,e]

[a] J. J. Hopfield and J. M. Worlock, Phys. Rev. 137, A1455 (1965).

[b] J. Ramamurti and K. Teegarden, Phys. Rev. 145, 698 (1966).

[c] J. W. Hodby, J. A. Borders, and F. C. Brown, Phys. Rev. Letters 19, 952 (1967).

[d] H. R. Philipp and H. Ehrenreich, Phys. Rev. 131, 2016 (1963).

[e] K. Teegarden and G. Baldini, Phys. Rev. 155, 896 (1967).

no one has yet calculated. The true excitonic series for $n \geq 2$ is expected to fit the hydrogenic case fairly well. For a discussion of the problems involved in determining a proper value for the dielectric constant as seen by the exciton (see Ref. 9).

M_h is determined from the table by the following relation:

$$R^* = \mu^*/\epsilon^2\mu \text{ Ry}$$

or

$$M_h = M_e(RM_e/\epsilon^2\mu R^* - 1)^{-1},$$

where Ry is the hydrogenic Ry equal to 13.6 eV; $R^* = E_B$; μ is the hydrogen reduced mass; and μ^* is the exciton reduced effective mass.

The hole effective mass was determined from other parameters since there are neither experimental values nor reliable theoretical calculations for it. Since small variations in variables, such as the dielectric constant and binding energy have an appreciable effect on M_h, its use here should be construed as instructive only.

*Research supported in part by the National Science Foundation.

[1] B. Segall, Phys. Rev. 150, 734 (1966).

[2] B. Segall and G. D. Mahan, Phys. Rev. 171, 935 (1968).

[3] R. J. Elliott, Phys. Rev. 108, 1384 (1957).

[4] H. Fröhlich, Advan. Phys. 3, 325 (1954).

[5] L. Hostler, J. Math. Phys. 5, 591 (1964).

[6] G. Baldini, A. Bosacchi, and B. Bosacchi, Phys. Rev. Letters 23, 846 (1969).

[7] Y. Toyazawa and J. Hermanson, Phys. Rev. Letters 21, 1637 (1968).

[8] K. Park and R. G. Stafford, Phys. Rev. Letters 22, 1426 (1969).

[9] R. S. Knox, *Theory of Excitons* (Academic, New York, 1963).

PHYSICAL REVIEW B VOLUME 3, NUMBER 8 15 APRIL 1971

Lattice Vibrations in Deuterated Ammonium Chloride at 85° K. I. Experimental*

H. C. Teh and B. N. Brockhouse
Department of Physics, McMaster University, Hamilton, Ontario, Canada
(Received 23 July 1970)

Dispersion curves for the [00ζ] (Δ), [ζζ0] (Σ), [ζζζ] (Λ), and [$\frac{11}{22}$ζ] (*T*) directions in ND_4Cl were measured at 85 °K by inelastic scattering of slow neutrons using the McMaster triple-axis crystal spectrometer at Chalk River. The single crystals were grown from solution. A torsional (librational) branch, flat within about 2%, with an average frequency of 8.3×10^{12} cps, was found. Results are compared with a modified rigid-ion-model calculation based on Parlinski's formulation. Symmetry points and branches in the dispersion curves are classified according to their symmetry species. The Lyddane-Sachs-Teller relation as generalized by Cochran holds within experimental accuracy.

I. INTRODUCTION

In this paper the results of a study of the lattice vibrations in deuterated ammonium chloride ND_4Cl at 85 °K by inelastic scattering of neutrons are given. A preliminary report has appeared.[1] An accompanying paper by Cowley[2] gives additional theoretical analysis.

ND_4Cl has a cubic structure; the Cl^- ion is located at the corner and the tetrahedral ND_4^+ ion at the body center of the cube, with the hydrogen atoms at tetrahedral positions along the body diagonals. Thus the ND_4^+ ion is immersed in an electric field produced by the eight nearest Cl^- ions. There are two possible orientations of the ND_4^+ ion such that the hydrogens always point towards the nearest Cl^- ions. At room temperature the crystal is in a disordered phase in that the ND_4^+ ions are randomly

TABLE I. Some properties of ND_4Cl and NH_4Cl.

ND_4Cl		
Lattice constant[a] (a)	3.8682 Å	(290 °K)
	3.8190 Å	(88 °K)
Density	1.6500 gm/cm^3	(290 °K)
	1.7146 gm/cm^3	(88 °K)
NH_4Cl		
Elastic constants[b] at 85 °K		
C_{11} (10^{11} dyn cm^{-2})	4.69 ± 0.05	
C_{44} (10^{11} dyn cm^{-2})	1.29 ± 0.02	
C_{12} (10^{11} dyn cm^{-2})	1.57 ± 0.07	
Static dielectric constant[c,d] (ϵ_s)	6.96	(300 °K)
Index of refraction[e] (n)	6.10 ± 0.10	(85 °K)
Optical frequency dielectric constant[f] (ϵ_∞)	1.6426	(300 °K)
	2.81	(85 °K)

[a] R. W. G. Wyckoff, *Crystal Structure* (Wiley, New York, 1963), Vol. I, p. 104.

[b] Extrapolated beyond 155 °K from Ref. 7.

[c] K. Højendahl, Kgl. Danske Videnskab. Selskab, Mat. Fys. Medd. No. 16, 115 (1938).

[d] Extrapolated beyond 173 °K from Ref. 8.

[e] J. R. Tessman, A. H. Kahn, and W. Shockley, Phys. Rev. 92, 890 (1953).

[f] Estimated from Ref. e of this table. See discussion in text.

distributed between these two orientations. The crystal undergoes[3] an order-disorder λ transition at 249.5 °K, below which the ND_4^+ ions are completely ordered. The space-group symmetry changes from O_h^1 ($Pm3m$) in the high-temperature phase to T_d^1 ($P\bar{4}3m$) in the low-temperature phase. Assuming the ammonium ions to be rigid, the dispersion curves in a general direction comprise nine external branches, corresponding to six degrees of freedom for the translational motions and three for the torsional (librational) motions. Investigations[4,5] of incoherent inelastic scattering by NH_4Cl have shown that a flat torsional branch exists having frequency 11.7×10^{12} cps. (Frequencies are given in units of 10^{12} cps throughout.) Incomplete measurements of the dispersion curves for NH_4Cl have been obtained[6] by Smith *et al.* using a triple-axis neutron spectrometer. We present here a complete set of dispersion curves $\nu(\vec{q})$ for the external translational and librational vibrations in the high-symmetry directions, measured using a large single crystal of ND_4Cl with a triple-axis spectrometer.

Some properties of ND_4Cl and NH_4Cl are given in Table I.

II. EXPERIMENTS AND RESULTS

ND_4Cl is chosen as the specimen instead of NH_4Cl because of the more favorable neutron properties of the former. The coherent scattering cross section for hydrogen[9] is only 1.79 b, whereas the incoherent cross section is 79.71 b. This means that a strong incoherently scattered neutron background would be found for NH_4Cl, including peaks at those frequencies corresponding to peaks in the frequency distribution. On the other hand, the coherent scattering cross section for deuterium is 5.4 b, while the incoherent cross section is only 2.2 b, a reasonably favorable condition for the present work.

The single-crystal specimens were grown from a saturated solution using a modified version of the Holden process.[10] The solution was prepared at 55 °C by adding ~ 550 g of NH_4Cl and ~ 180 g of urea to 750 cm^3 of D_2O. The solvent was then removed by evaporation, and ~ 350 cm^3 of fresh D_2O was added; the solution was then allowed to stay for ~ 24 h at 55 °C for further deuteration. This process was repeated six times. The addition of urea is necessary as a habit modifier to prevent irregular growth and also to promote growth of large single crystals. The solution was left in a sealed beaker. Once the crystallization temperature was determined, the beaker was immersed in a temperature controlled bath (with ± 0.1 °C fluctuation) and the solvent was allowed to evaporate slowly under a pressure ~ 50 cm of Hg as the temperature was lowered at a rate ranging from 0.1 °C per day to 0.5 °C per day. The largest crystal thus obtained is ~ 30 cm^3 ($2.5\times3.3\times3.6$ cm^3) with (100) cubic faces. The size of the crystal being used (after cutting) is about 12 cm^3 ($1.0\times3.3\times3.6$ cm^3).

The degree of deuteration was determined by a density measurement. Small pieces of single crystal cleaved from the largest crystal used were placed in a mixture of heavy organic solutions (carbon tetrachloride CCl_4 and ethylene bromide CH_3CHBr). The density of the solution was adjusted until the crystals started to float. Further fine adjustment allowed the crystals to float in the solution. The density of the solution was then accurately measured by a specific-gravity bottle. Both the densities of the specimens and of NH_4Cl crystals were noted. Taking the density to be the total weight of a ND_4Cl molecule divided by the unit-cell volume, the deuteration is found to be only 95 ± 2%. Estimates of the deuteration from the incoherent elastic scattering and from the transmission of neutrons agreed with this figure. The mosaic spread of the specimen was measured by rocking the specimen orientation with respect to the incident neutron beam, and was found to be about 0.4° full width at half-maximum (FWHM).

The experiments were carried out on the McMaster triple-axis crystal spectrometer[11] at the NRU reactor of the Chalk River Nuclear Laboratories. The measurements were carried out for wave vectors in the (100) and (1$\bar{1}$0) planes of the crystal,

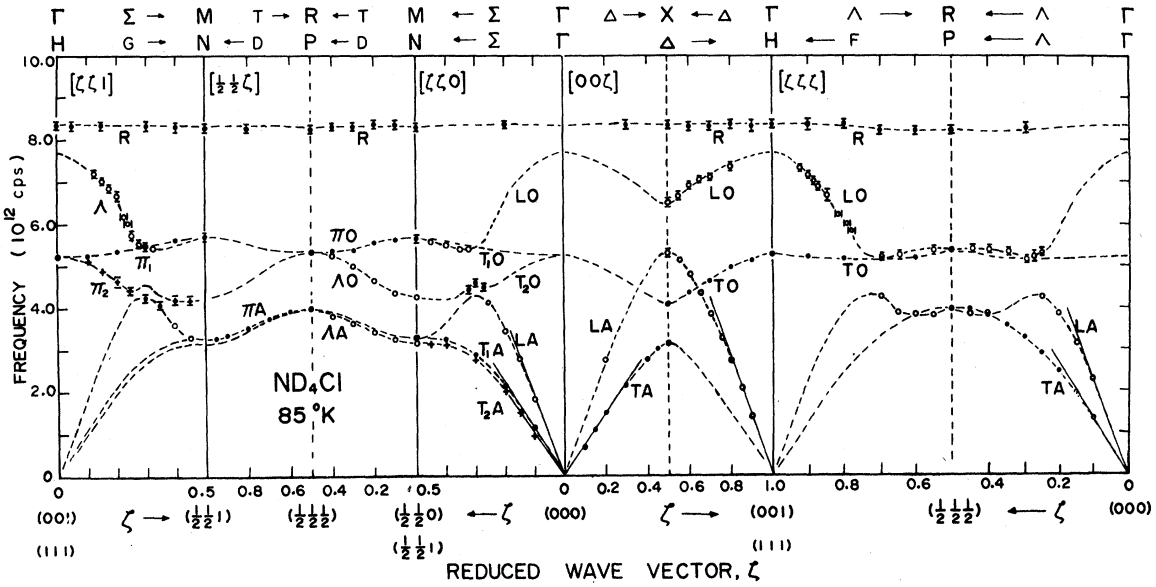

FIG. 1. Dispersion curves with (dashed) guidelines for ND_4Cl in the symmetry directions at 85 °K. The diagram is labeled with the group-theoretical notation of Koster (Ref. 13). The straight lines through the points Γ give the initial slopes of the dispersion curves as calculated from the elastic constants given in Table I. The reduced wave vector $\vec{\zeta} = a\vec{q}/2\pi$, where $\vec{q}$ is the quasimomentum of the phonon. ○ denotes longitudinal and Λ modes; + and ●, transverse and π modes; and ■, uncertain modes.

normally using the "constant-$\vec{Q}$" method.[12]

The over-all shape of the dispersion curves measured at 85 °K is shown in Fig. 1 (the dotted lines are guidelines). Plotting of the dispersion curves in this manner provides general information for the structure factor. The phonons (neutron groups) are then actually observed at those positions in reciprocal space at which they are plotted in Fig. 1. The definition of the structure factor will be discussed later. If the ND_4^+ and Cl^- ions were treated alike, the body-centered cubic (bcc) structure would be appropriate.[14] In this way the optical branches are to be measured around those reciprocal-lattice (RL) points which are not RL points for the bcc lattice. Figure 2 shows the $(1\bar{1}0)$ plane of the reciprocal lattice for both structures. For the bcc structure, the Brillouin-zone boundaries are indicated by heavy lines, the RL points and the symmetry points and lines are indicated by large numbers and letters, respectively, while the light lines and small letters are for simple cubic structure. Being restricted by the structure factor, the appropriate positions in the reciprocal space for the measurement of the optical branches (LO, T_1O, and T_2O) along the $[\zeta\zeta 0]$ direction are now chosen along the $[\zeta\zeta 1]$ direction at points which would be labeled Λ, π_1, and π_2 in the bcc structure. Moreover, in the $[\zeta\zeta 0]$ direction the structure factors for the LA and LO branches interchange roles beyond $\zeta \sim 0.3$ at which point the two longitudinal branches split. Similar behavior occurs along the $[\zeta\zeta\zeta]$ di-

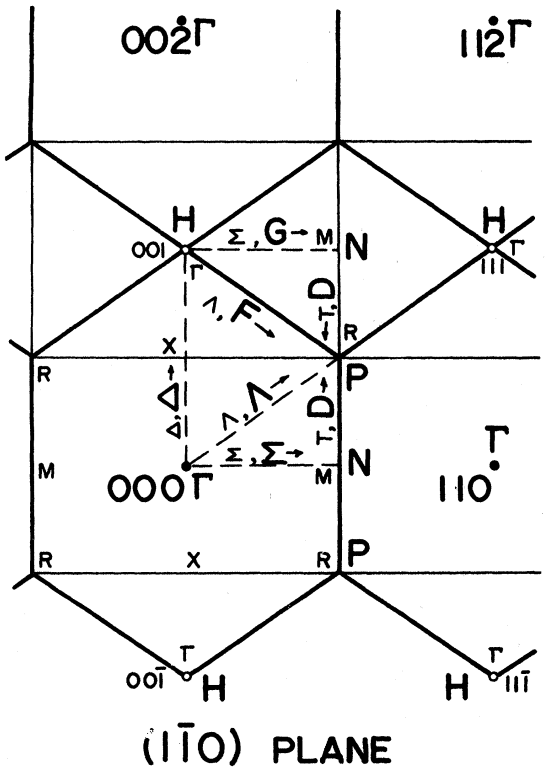

FIG. 2. $(1\bar{1}0)$ plane of the reciprocal lattice for ND_4Cl showing the description for the bcc as well as the simple cubic Brillouin zones (see detailed description in text).

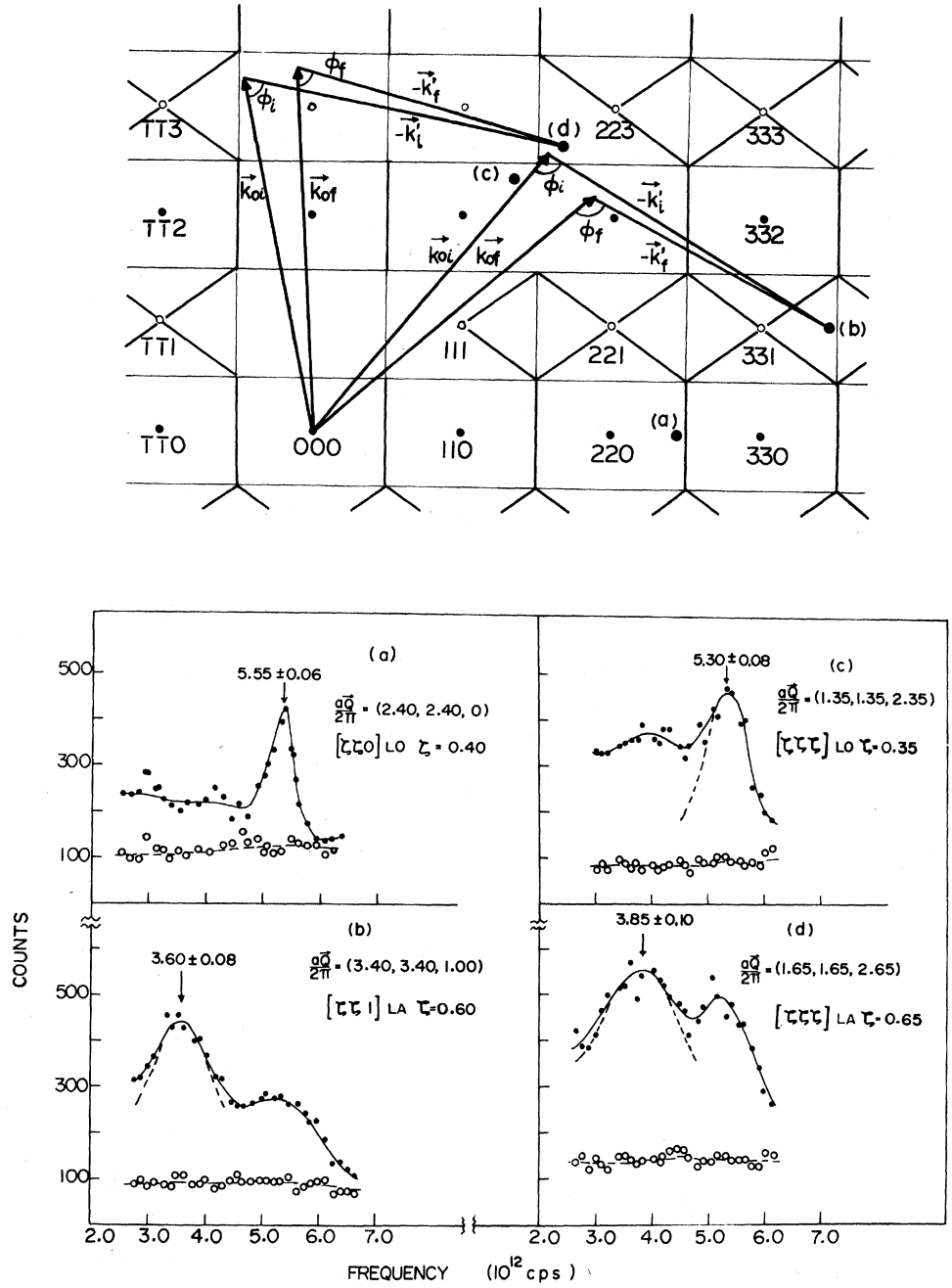

FIG. 3. Upper part of the diagram shows the $(1\bar{1}0)$ plane of the reciprocal lattice for ND_4Cl illustrating how the longitudinal phonons [(a) and (b) in the [ζζ0] direction; (c) and (d) in the [ζζζ] direction] are measured in the "constant-$\vec{Q}$" experiments. $\vec{k}_0$ and $\vec{k}'$ are the incident and scattered neutron wave vectors, respectively, ϕ is the scattering angle. $\vec{Q} = \vec{k}_0 - \vec{k}'$ is the momentum transfer. The subscripts i and f denote the initial and final values, respectively, for each variable during a scan. The corresponding neutron groups in the lower part of the diagram are labeled with branch designations. Signal counts are indicated by filled circles and background counts by open circles. (This convention also applies to Figs. 5 and 6.)

rection. Figure 3 illustrates the way some of these longitudinal modes were measured together with the corresponding neutron groups. The lines through the points are drawn by hand and do not represent any fitting procedure. Figure 4 presents the same results as Fig. 1 for the usual symmetry directions of the actual cubic cell.

The Debye-Waller factor of the ND_4^+ ion is small at large momentum transfer $\vec{Q}$. Therefore it is not advisable to use a large value of $\vec{Q}$ for the mea-

surements of some phonons. For example, the Debye-Waller factor of the hydrogens at room temperature[5] is about 0.7 at the RL point (1, 1, 1), but only about 0.07 at (3, 3, 3). Moreover, the presence of the deuterium atoms introduces an extra parameter in the structure factor so that a reduced structure factor cannot be defined as in the case of simple crystals.

Some of the typical neutron groups are shown in Fig. 5. A neutron group of frequency 9.2 was observed in the first specimen (along with the torsional mode R at 8.3 frequency units); this group is attributed to a defect torsional mode arising from the presence of ND_3H^+ defect ions in the specimen and will be discussed later. To study the torsional mode in detail, a second specimen (deuteration $99 \pm 1\%$) was grown. The size is about 6.5 cm^3 ($1.0 \times 2.5 \times 2.6$ cm^3) with a mosaic spread of about 0.3° FWHM. Figure 6 compares the torsional modes Γ_{25} measured at the same RL point (3, 3, 2) in both specimens. Specimen II shows only the pure torsional mode as it should.

Table II gives the complete list of frequencies with estimated errors. The errors assigned to the measured frequencies are generally one-tenth of the FWHM. In a few cases where poor groups only are available, the frequencies were averaged over several groups obtained at equivalent reduced wave vectors with larger assigned errors.

III. DISCUSSION

As is pointed out earlier, the bcc structure would be appropriate had the Cl^- and ND_4^+ ions been alike, in which case the TO and LO frequencies at Γ would be degenerate, and also the gaps developed between TA and TO and between LA and LO branches at the symmetry point X would disappear. But in the actual case, these degeneracies are lifted, respectively, because of the presence of electric charges and of the other differences between the ions.

A symmetry table showing the compatibility relations and the modes of vibration of the ions (the corresponding symmetry modes) is given, in an accompanying paper,[2] by Cowley. According to the symmetry properties of the crystal the LO and LA branches in both $[\zeta\zeta 0]$ and $[\zeta\zeta\zeta]$ directions should not cross (as is shown in Fig. 1) since these transform according to the same representation. The T_2O and LA branches in the $[\zeta\zeta 0]$ direction also transform according to the Σ_1 representation, and thus develop a small energy gap. However, the crossing of these two branches is allowed in the disordered phase, in which they are

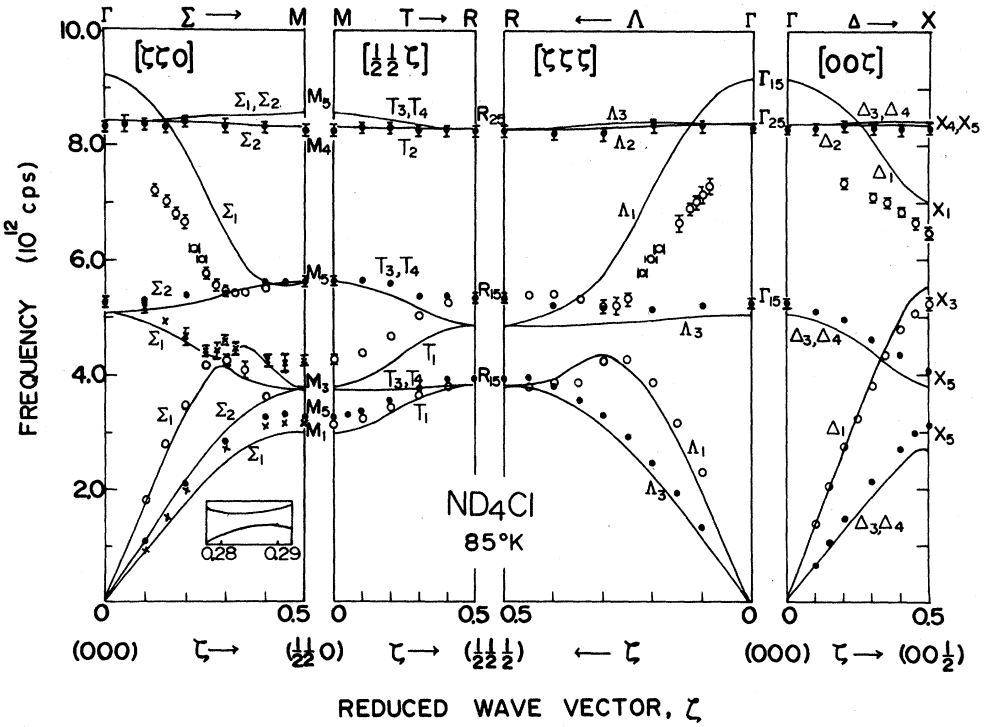

FIG. 4. Dispersion curves for ND_4Cl at 85 °K for the usual symmetry directions of the actual cubic cell. The solid lines are a modified rigid-ion-model calculation based on Parlinski's formulation (Ref. 15). The parameters of the model were determined from other data as discussed in the text. The group theoretical notations are assigned to the branches according to their eigenvectors.

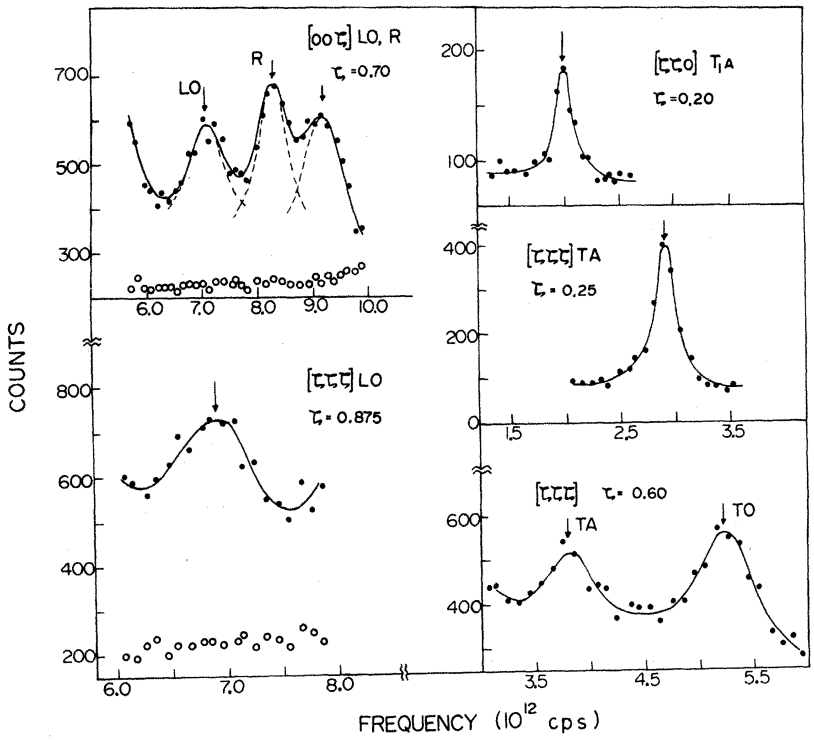

FIG. 5. Some typical neutron groups for ND_4Cl at 85 °K obtained in "constant-$\vec{Q}$" experiments.

truly transverse and longitudinal, and transform according to different representations. The polarization of phonons in this region of small energy splitting is not uniquely prescribed by the experiments and the phonons are therefore indicated by square dots in Fig. 1.

The energy gaps developed between the longitudinal branches along the Δ, Σ, and Λ directions are about 1 frequency unit; the splittings occur at $\vec{q}$ in the region from 0.45 to 0.5 (in units $2\pi/a$). These gaps might be expected to show some temperature dependence, especially through the transition region, and will be studied further.

A calculation based on Parlinski's modification[15] of the rigid-ion model is shown in Fig. 4. In general a large number of force constants are required to describe the lattice dynamics. In this model there are 18 force constants, eight of which are obtained from an electrostatic model in which the NH_4^+ ion is approximated by four electronic charges, each $+\frac{1}{4}e$, situated at the hydrogen positions, with charge $-e$ at the Cl^- positions. The rest of the force constants are derived from the experimental elastic constants through the method of long waves, from the frequency ($\nu = 11.8$) of the torsional mode as determined by neutron incoherent scattering, and from the frequency[3] ($\nu = 5.54$) of the TO mode at $\vec{q} = 0$ as determined by infrared absorption. These five experimental data enable only five of the ten unknown force constants to be determined. The remaining five are eliminated by assuming that the short-range interactions between the nearest Cl^--Cl^- and NH_4^+-NH_4^+ ion pairs are equal, and that the interactions between the nearest Cl^--NH_4^+ ion pair along the [111] and $[\bar{1}\bar{1}\bar{1}]$ directions are identical. With this five-parameter model, Parlinski predicted the dispersion curves for NH_4Cl; the curves have the general shape of the experimental ones for ND_4Cl, but quantitatively the agreement is poor. In the present calculation, using numerical values appropriate to ND_4Cl, the agreement is only slightly improved.[16] The group-theoretical notations are assigned to the branches according to their eigenvectors and the compatibility relations. (The eigenvectors are linear combinations of the symmetry modes.) The classification of those phonons into the transverse and longitudinal modes in the branch-mixing region along the Σ direction is based on symmetry arguments and on the fact that the model calculation does show a frequency gap between the two Σ_1 branches.

The splitting of the torsional mode at M into M_4 and M_5 was verified by measurements at two different positions in reciprocal space: One, assigned as M_4, with frequency 8.1 ± 0.10 was measured at (1.5, 1.5, 4.0), and the other, assigned as M_5, with frequency 8.40 ± 0.08 at (3.5, 3.5, 1.0). They are not shown in the figure. The detailed dispersion relation of the torsional modes along this direction will be studied further.

In molecular crystals we may assume that there

are modes in which molecules move almost as rigid units. The structure factor $G_j(\vec{Q})$ of the one-phonon process for these corresponding modes, is given by the following expression[17]:

$$|\vec{Q}|\,G_j(\vec{Q}) = \sum_{K,p} f_p \vec{Q}\cdot[\hat{\xi}(s,K) + \hat{\theta}(s,K)\times\vec{R}_p] \times e^{-W_p(\vec{Q})}\, e^{i\vec{Q}\cdot\vec{R}_p}\, e^{i\vec{\tau}\cdot\vec{R}_K}\,, \quad (1)$$

where $\vec{\tau}=\vec{Q}+\vec{q}$ is a RL vector; f_p and W_p are the atomic scattering and Debye-Waller factors, respectively, for the pth atom of the Kth molecule; $\vec{R}_p$ is the position of the pth atom relative to the center of mass of the molecule K; $\vec{R}_K$ is the center of mass of the Kth molecule relative to the origin of the cell; $\hat{\xi}(s,K)$ and $\hat{\theta}(s,K)$ are the translational and torsional eigenvectors of the $s\equiv(j,\vec{q})$ mode (j is the branch index) for molecule K.

In the case of crystals without "rigid" molecular groups the index K identifies only an atom rather than a molecule, and the structure factor reduces to

$$|\vec{Q}|\,G_j(\vec{Q}) = \sum_K f_K \vec{Q}\cdot\vec{\xi}(s,K)\, e^{-W_K(\vec{Q})}\, e^{i\vec{\tau}\cdot\vec{R}_K}\,. \quad (2)$$

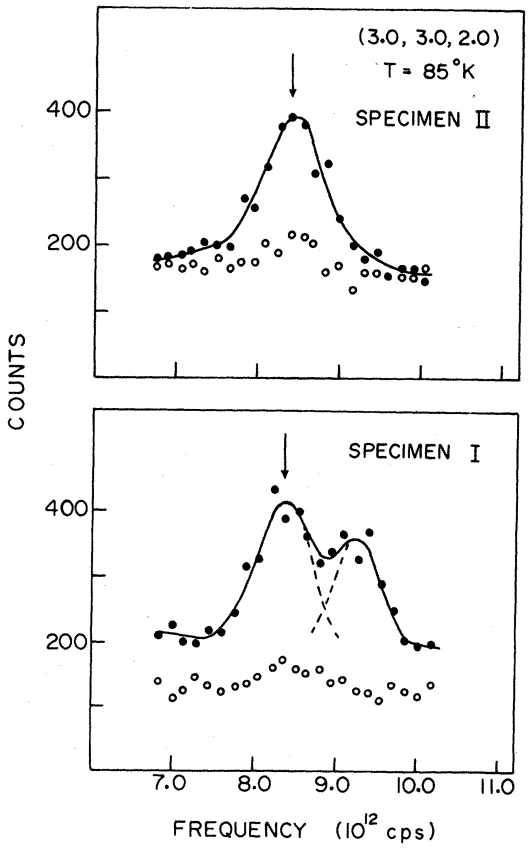

FIG. 6. Comparison of the torsional mode Γ_{25} ($\nu = 8.35\times10^{12}$ cps) measured at (3, 3, 2) in the two specimens indicating the presence of the defect torsional mode ($\nu = 9.20\times10^{12}$ cps) in specimen I.

Thus the structure factor can be calculated, provided the eigenvectors of the various modes for the individual atoms are known. In our calculation we take[13]

$$f_K \sim (M_K\omega_s)^{-1/2} b_K\,,$$

where M_K and b_K are the mass and scattering length of the Kth atom, and ω_s is the frequency of the sth mode.

The intensity of the neutron group is thus proportional to the square of the structure factor. A calculation based on the above rigid-ion model was carried out. This calculation acts only as a rough guide to some of the phonon measurements. It does not predict the irregular behavior of the structure factor for the LA mode in the $[00\zeta]$ direction in which the LA branch is better measured from $\zeta = 0.5$ to $\zeta = 1.0$ instead of from $\zeta = 0.0$ to $\zeta = 0.5$. The structure factor alone is not sufficient to identify those phonons in the branch-mixing region in the $[\zeta\zeta 0]$ direction, since the polarization vectors (or eigenvectors) for those atoms involved in these modes given by the calculation are very sensitive to the details of the calculation and in general are neither longitudinal nor transverse. Therefore the symmetry properties of the crystal were used to aid the identification of those phonons in this region, keeping in mind that branches which transform according to the same representation normally do not cross.

The LO frequency at Γ is not obtained, partly because the intensity of the LO mode is weaker than that of the torsional mode and also because each neutron group has a width of 1.0 while their separation is only about 0.6. Nevertheless it is still well defined by the three slopes of the LO branches and is estimated to be 7.7 ± 0.15. The TO frequency at Γ is 5.25 ± 0.06.

The original Lyddane-Sachs-Teller (LST) relation was derived for diatomic diagonally cubic crystals (alkali halides).[18] For crystals having orthorhombic symmetry or higher with more than two atoms per primitive cell, the generalized LST relation was shown by Cochran[19,20] to be

$$\Pi_n\,(\omega_n^2)_L/(\omega_n^2)_T = \epsilon_s/\epsilon_\infty\,. \quad (3)$$

ϵ_s and ϵ_∞ are the static and high (optical) frequency dielectric constants, $(\omega_n)_L$ and $(\omega_n)_T$ are the angular frequencies of the longitudinal and transverse modes, respectively; at long-wavelength limit, the index n runs over all the polarized optically active modes. There are three such paris of active modes in ND_4Cl: one external mode and two internal modes. The two internal modes were observed[3,21] earlier for NH_4Cl using infrared absorption. A complete set of frequencies for the internal modes of NH_4Cl obtained from both infrared and Raman measurements was recently given by Schumaker

TABLE II. Phonon frequencies (in units of 10^{12} cps) of ND_4Cl at 85 °K with estimated errors. $\zeta = aq/2\pi$.

ζ	ν(Acoustic)	ν(Optic)	ζ	ν(Acoustic)	ν(Optic)
		[00ζ] T			
0.10	0.65 ± 0.05		0.50		4.07 ± 0.04
0.15	1.06 ± 0.02		0.60		4.34 ± 0.06
0.20	1.49 ± 0.01		0.70		4.62 ± 0.08
0.30	2.14 ± 0.01		0.80		4.95 ± 0.06
0.40	2.71 ± 0.01		0.90		5.10 ± 0.06
0.45	3.00 ± 0.04		1.00		5.25 ± 0.06
0.50	3.14 ± 0.04				
		[00ζ] L			
0.20	2.75 ± 0.08		0.70	3.84 ± 0.03	7.10 ± 0.08
0.50	5.25 ± 0.07	6.50 ± 0.08 [a]	0.75	3.25 ± 0.04	
0.55	5.10 ± 0.06	6.66 ± 0.10	0.80	2.75 ± 0.05	7.35 ± 0.10
0.60	4.78 ± 0.08	6.85 ± 0.05	0.85	2.06 ± 0.03	7.50 ± 0.15
0.65	4.34 ± 0.04	7.02 ± 0.08	0.90	1.39 ± 0.06	
			1.00		(7.70 ± 0.15) [b]
		[00ζ] R			
0.50		8.30 ± 0.07	0.80		8.35 ± 0.10
0.60		8.30 ± 0.10	0.90		8.30 ± 0.10
0.70		8.30 ± 0.10	1.00		8.35 ± 0.10 [a]
0.20		8.30 ± 0.10 [a]			
		[$\zeta\zeta$0] T_1A, π_1			
0.10	1.07 ± 0.01		0.60		5.60 ± 0.06
0.20	2.09 ± 0.03		0.70		5.44 ± 0.06
0.30	2.83 ± 0.03		0.80		5.36 ± 0.06
0.40	3.25 ± 0.06		0.90		5.28 ± 0.06
0.50	3.25 ± 0.04				
		[$\zeta\zeta$0] T_2A, π_2			
			0.50		4.25 ± 0.07
0.10	0.91 ± 0.02		0.55		4.20 ± 0.15
0.15	1.52 ± 0.03		0.60		4.25 ± 0.12
0.20	1.99 ± 0.02		0.70		4.25 ± 0.08
0.30	2.74 ± 0.04		0.75		4.40 ± 0.10
0.40	3.10 ± 0.05		0.80		4.65 ± 0.15
0.45	3.14 ± 0.05		0.85		4.90 ± 0.06
0.50	3.15 ± 0.03		0.90		5.15 ± 0.10
		[$\zeta\zeta$0] L, Λ			
0.10	1.80 ± 0.08		0.65	4.10 ± 0.10	
0.15	2.78 ± 0.05		0.675		5.42 ± 0.08
0.20	3.44 ± 0.05		0.70		5.45 ± 0.08
0.25	4.13 ± 0.08		0.725		5.55 ± 0.10
0.30	4.60 ± 0.08		0.750 ± 0.06 [c]		6.029
0.325	4.45 ± 0.10	5.40 ± 0.10	0.770 ± 0.04 [c]		6.232
0.35		5.40 ± 0.05			
0.40		5.55 ± 0.06 [a]	0.775		6.25 ± 0.15
0.45		5.60 ± 0.05	0.80		6.65 ± 0.10
0.50		5.62 ± 0.06	0.825		6.80 ± 0.10
0.55	3.30 ± 0.06		0.85		7.00 ± 0.10
0.60	3.60 ± 0.08		0.875		7.20 ± 0.10
		[$\zeta\zeta$0] R			
0.50		8.10 ± 0.10 [a]			
0.50		8.40 ± 0.08 [a]	0.85		8.30 ± 0.10
0.60		8.30 ± 0.10	0.90		8.35 ± 0.10
0.70		8.30 ± 0.15	0.95		8.35 ± 0.15
0.80		8.40 ± 0.10	0.20		8.35 ± 0.08 [a]

TABLE II. (*continued*).

ζ	ν(Acoustic)	ν(Optic)	ζ	ν(Acoustic)	ν(Optic)
		[$\zeta\zeta\zeta$] T			
0.10	1.32±0.03		0.45	3.95±0.03	
0.15	1.93±0.02		0.50	3.92±0.06	5.32±0.08
0.20	2.46±0.01		0.60		5.20±0.06
0.25	2.90±0.02		0.70		5.16±0.06
0.30	3.27±0.03		0.80		5.14±0.06
0.35	3.56±0.03		0.90		5.20±0.08
0.40	3.80±0.05				
		[$\zeta\zeta\zeta$] L			
0.10	2.28±0.04		0.65	3.85±0.10	5.30±0.10
0.15	3.14±0.04		0.70	4.25±0.10	5.15±0.10
0.20	3.86±0.04		0.785±0.06[c]		5.815
0.25	4.26±0.08				
0.30	4.25±0.07	5.15±0.10	0.795±0.05[c]		6.000
0.35		5.30±0.08	0.820±0.06[c]		6.232
0.40	3.85±0.10	5.40±0.10	0.85		6.65±0.15
0.45	3.84±0.08	5.40±0.08	0.875		6.90±0.10
0.50	3.92±0.06	5.32±0.08	0.90		7.15±0.15
0.55	3.80±0.06	5.35±0.10	0.9125		7.30±0.15
0.60	3.85±0.06				
		[$\zeta\zeta\zeta$] R			
0.50		8.15±0.12[a]	0.80		8.35±0.10
0.60		8.20±0.10	0.90		8.35±0.15
0.70		8.25±0.10[a]	0.30		8.25±0.12[a]
		[1/21/2ζ] π			
0.10	3.30±0.03	5.62±0.06	0.70	3.75±0.08	
0.20	3.52±0.05	5.56±0.06	0.80	3.52±0.06	5.60±0.08
0.30	3.70±0.04	5.35±0.06	0.90	3.34±0.06	
0.40	3.90±0.06	5.35±0.05	0.95	3.28±0.05	
0.60	3.90±0.08				
		[1/21/2ζ] Λ			
0.10	3.25±0.06	4.35±0.05	0.30	3.65±0.15	4.97±0.06
0.20	3.45±0.06	4.65±0.05	0.40	3.80±0.06	5.25±0.06
		[1/21/2ζ] R			
0.10		8.30±0.10	0.30		8.25±0.10
0.20		8.30±0.10	0.40		8.25±0.10
0.80		8.20±0.08[a]			

[a]Measurements using the second specimen.
[b]Estimated from the three slopes of the LO branches.
[c]Constant E measurements.

et al.[22] The frequencies are $\nu_L = 42.60$ and $\nu_T = 42.09$ for the bending mode $\nu_4(F_2)$, $\nu_L = 94.14$ and $\nu_T = 93.78$ for the stretching mode $\nu_3(F_2)$. Furthermore, the shell-model calculation of Cowley[2] for ND_4Cl in the accompanying paper gives $\nu_L = 33.13$, $\nu_T = 32.76$, $\nu_L = 69.57$, $\nu_T = 69.51$. Thus, after accounting for the correction for the internal optically active modes, the LST relation reduced to

$$(\omega_L/\omega_T)^2 = 0.969\,(\epsilon_s/\epsilon_\infty)\,, \tag{4}$$

where ω_L and ω_T are the angular frequencies of the external longitudinal and transverse modes.

From the present measurements we have $(\omega_L/\omega_T)^2 = 2.14 \pm 0.10$, taking into account the errors of ω_L and ω_T mentioned above. To obtain the dielectric constant ratio we first estimate the value of ϵ_∞ at 85 °K from the value measured at room temperature. From Table I it may be estimated that the decrease in the lattice constant of ND_4Cl as the temperature is lowered from room temperature to 85 °K is about 1.4%. This 4.2% decrease in volume of the unit cell causes an increase in the number of molecules per unit volume, thus changing ϵ_∞ the dielectric constant for optical frequency. The shift in ϵ_∞ can be estimated from the Clausius-Mossotti relation as follows: Assuming

that the electronic polarizabilities for each ion remain constant over the same temperature range, the change in the volume of the unit cell by -4.2% produces a shift in ϵ_∞ by about $+4.1\%$. Using the extrapolated value of the static dielectric constant ϵ_s at 85 °K from Table I, we find $\epsilon_s/\epsilon_\infty = 2.17 \pm 0.08$ (allowing for about 3.5% error in the estimation and the extrapolation). Thus the right-hand side of Eq. (4) becomes 2.11 ± 0.07 after taking into account the correction for the internal modes. Assuming that the difference between the dielectric constants of ND_4Cl and NH_4Cl is negligible, the LST relation holds in ND_4Cl within experimental accuracy. Moreover, it is worthwhile to note that the defect ions ND_3H^+ (about 5%) in the specimen might be slightly deformed and contribute to the polarization. On the other hand, the possibility of contamination from OH^- ions and H_2O molecules was not taken into account in the dielectric-constant measurements of NH_4Cl, though the effect is probably only important below liquid-nitrogen temperature as illustrated by measurements[23,24] on alkali halides.

The torsional mode is flat within about 2% with an average frequency 8.3. This flatness implies that interaction between the tetrahedra is small. (The interaction cannot be zero because then no ordering would occur at the transition.)

Neutron groups with a frequency 9.2 were also found at symmetry points and elsewhere in the zone. These are ascribed to defect torsional modes involving ND_3H^+ ions; they are visible because of the large incoherent scattering cross section of hydrogen and the extreme flatness of the R branch. As a result of the 5% hydrogen which remained in the crystal, the principal defect ions are of the form ND_3H^+; these have two of their principal moments of inertia smaller than those of ND_4^+ ions by a factor of 0.812, with the third unchanged. (The latter is not involved in motion of the hydrogens, however, and is thus not active.) Consequently the defect torsional frequency is 9.2 instead of 8.3. This group is in fact always seen with about the expected intensity.

The above interpretation of the defect mode in the first specimen is confirmed by the fact that the defect mode disappears in the second specimen as indicated in Fig. 6. On the other hand, within experimental accuracy, the translational modes are not affected by the 5% hydrogen retained in the rst specimen.

It is a familiar fact that the limiting slopes of the acoustical branches at zero wave vector corresponding to the appropriate sound velocities are related to the elastic constants and the density of the crystal (except for effects of the difference between zeroth and first sound[25]). Using extrapolated values of elastic constants, given for NH_4Cl in Table I, slopes were obtained as shown in Fig. 1. Within the accuracy of our measurements and the estimated errors in the extrapolated values of the elastic constants at 85 °K, the agreement is satisfactory.

Finally, as is shown in Fig. 1, there exist fairly flat branches in the frequencies ranging from 4.0 to 5.5 in addition to the flat torsional branches. These frequencies should show up as peaks in the frequency distribution.

It is intended to continue the experiments to study the behavior of the phonons with temperature through the λ transition. Preliminary work has been done at room temperature which indicates a significant frequency shift in the acoustical branches and considerable broadening of the neutron groups in the torsional branches.

ACKNOWLEDGMENTS

The authors wish to express their appreciation to the National Research Council of Canada for financial support, to the staff of the Atomic Energy of Canada Ltd. at Chalk River for their cooperation, and in particular to Dr. G. Dolling and Dr. B. M. Powell for a helpful discussion. We wish to thank Dr. E. R. Cowley and Dr. G. A. deWit for many discussions; both participated in various ways in the over-all project.

---

*Work supported by the National Research Council of Canada.

[1]H. C. Teh, B. N. Brockhouse, and G. A. DeWit, Phys. Letters 29A, 694 (1969).

[2]E. R. Crowley, following paper, Phys. Rev. B 3, 2743 (1971).

[3]E. L. Wagner and D. F. Hornig, J. Chem. Phys. 18, 296 (1950).

[4]A. D. B. Woods, B. N. Brockhouse, M. Sakamato, and R. N. Sinclair, in *Inelastic Scattering of Neutrons in Solids and Liquids* (International Atomic Energy Agency, Vienna, 1961), p. 487.

[5]G. Venkataraman, K. Usha Deniz, P. K. Iyengar, A. P. Roy, and P. R. Vijayaraghavan, J. Phys. Chem. Solids 27, 1103 (1966).

[6]H. G. Smith, J. G. Traylor, and W. Reichardt, Phys. Rev. 181, 1218 (1969); and (private communication).

[7]C. W. Garland and R. Renard, J. Chem. Phys. 44, 1130 (1966).

[8]K. Kamiyoshi, Sci. Res. Inst. (Tohoku Univ.) A8, 252 (1956).

[9]D. J. Hughes and R. B. Schwartz, *Neutron Cross Sections, Brookhaven National Laboratory Report No.* 325, 2nd ed. (U. S. GPO, Washington, D. C., 1958).

[10]A. N. Holden, Discussions Faraday Soc. 5, 312 (1949).

[11]B. N. Brockhouse, G. A. DeWit, E. D. Hallman, and J. M. Rowe, in *Neutron Inelastic Scattering Vol.* II (International Atomic Energy Agency, Vienna, 1968), p. 259.

[12]E. C. Svensson, B. N. Brockhouse, and J. M. Rowe, Phys. Rev. 155, 619 (1967).

[13]G. F. Koster, in *Solid State Physics*, edited by

F. Seitz and D. Turnbull (Academic, New York, 1957), Vol. 5, p. 173.

[14]B. N. Brockhouse, in *Phonons in Perfect Lattices and Lattices with Point Imperfections*, edited by R. W. H. Stevenson (Oliver and Boyd, Edinburgh, 1966), p. 110.

[15]K. Parlinski, Acta Phys. Polon. 34, 1019 (1968); 35, 223 (1969).

[16]We received also a copy of Parlinski's calculations for ND_4Cl after making the above calculation. Our calculations show the splitting of the two Σ_1 branches (LA and T_2O) in the [ζζ0] direction. The gap is very small and is illustrated in the inset of Fig. 4. The $\Sigma_1(LO)$ and $\Sigma_2(T_1O)$ branches are also degenerate at the point M_5 as should be the case by symmetry.

[17]W. Cochran and G. S. Pawley, Proc. Roy. Soc. (London) A280, 1 (1964).

[18]R. H. Lyddane, R. G. Sachs, and E. Teller, Phys. Rev. 59, 673 (1941).

[19]W. Cochran, Z. Krist. 112, 30 (1959).

[20]W. Cochran and R. A. Cowley, J. Phys. Chem. Solids 23, 447 (1962).

[21]C. W. Garland and N. E. Schumaker, J. Phys. Chem. Solids 28, 799 (1967).

[22]N. E. Schumaker and C. W. Garland, J. Chem. Phys. 53, 392 (1970).

[23]R. P. Lowndes and D. H. Martin, Proc. Roy. Soc. (London) A308, 473 (1969).

[24]M. C. Robinson and A. C. H. Hallett, Can. J. Phys. 44, 2211 (1966).

[25]R. A. Cowley, Proc. Phys. Soc. (London) 90, 1127 (1967).

PHYSICAL REVIEW B VOLUME 3, NUMBER 8 15 APRIL 1971

Lattice Vibrations in Deuterated Ammonium Chloride at 85 °K. II. Theoretical*

E. R. Cowley
Department of Physics, McMaster University, Hamilton, Ontario, Canada
(Received 23 July 1970)

A shell model is shown to provide a good fit to the phonon dispersion curves in ND_4Cl. The model contains 22 parameters of which 13 are fitted to the experimental measurements. The ionic charge on the chlorine, and the electronic polarizabilities of the ions, are not fitted to the experiments. The ND_4 group is not treated as rigid, but it is shown that an effective dynamical matrix can be set up, which does not contain the internal coordinates explicitly, but which describes their effect on the external dispersion curves to a very good approximation. The dispersion curves in NH_4Cl are also calculated. A group-theoretical analysis of the symmetry of the normal modes is given in the Appendix.

I. INTRODUCTION

In the preceding paper[1] the phonon dispersion curves in the ordered phase of deutero-ammonium chloride, ND_4Cl are described and compared with theoretical curves, calculated by Parlinski,[2] based on the rigid-ion and rigid-molecule approximations. A number of discrepancies exist between the experimental and calculated curves, and it is not possible *a priori* to absolve either of the above approximations. In this paper we describe a model which contains neither approximation, and which provides a satisfactory description of the experimental curves.

The most straightforward method of including all of the effects required is to abandon the concept of the ND_4 ion as a useful unit and to regard the unit cell as containing six independent atoms or ions. This is the approach initially adopted here. The polarizabilities of the ions are taken into account in the shell-model formalism.[3,4] A shell model containing simplifications appropriate to ND_4Cl is described in Sec. II, and the results of a least-squares fit to the experimental data are given in Sec. III. The model contains 22 parameters, but the values of some of them can be deduced from other data, and a model in which 13 of the parameters are adjusted to fit the phonon dispersion curves provides satisfactory agreement with experiment.

The procedure described above is the safest way of ensuring that all of the effects associated with both ionic and molecular polarizability are included, but it does not contain the intuitively appealing separation of the dispersion curves into external and internal branches. In Sec. IV we describe an approximation to the dynamical matrix in which the internal coordinates of the ND_4 group are eliminated from the equation for the external branches, but the effects of the internal deformations on the external branches are well represented.

Some of the features of the model are discussed in Sec. V, and the model is also used to predict the form of the dispersion curves in NH_4Cl.

II. SHELL-MODEL FORMALISM

The equations of motion of the shell model can be written in the form[3,4]

$$\underline{m}\omega^2\underline{U} = (\underline{R} + \underline{ZCZ})\underline{U} + (\underline{T} + \underline{ZCY})\underline{W},$$